



**Discover Generics**

Cost-Effective CT & MRI Contrast Agents

**FRESENIUS  
KABI**

[WATCH VIDEO](#)

**AJNR**

This information is current as  
of June 13, 2025.

**Lateral Decubitus Dynamic CT Myelography  
with Real-Time Bolus Tracking (dCTM-BT)  
for Evaluation of CSF-Venous Fistulas:  
Diagnostic Yield Stratified by Brain Imaging  
Findings**

Thien J. Huynh, Donna Parizadeh, Ahmed K. Ahmed,  
Christopher T. Gandia, Hal C. Davison, John V. Murray, Ian  
T. Mark, Ajay A. Madhavan, Darya Shlapak, Todd D.  
Rozen, Waleed Brinjikji, Prasanna Vibhute, Vivek Gupta,  
Kacie Brewer and Olga Fermo

*AJNR Am J Neuroradiol* 2024, 45 (1) 105-112

doi: <https://doi.org/10.3174/ajnr.A8082>

<http://www.ajnr.org/content/45/1/105>

# Lateral Decubitus Dynamic CT Myelography with Real-Time Bolus Tracking (dCTM-BT) for Evaluation of CSF-Venous Fistulas: Diagnostic Yield Stratified by Brain Imaging Findings

Thien J. Huynh, Donna Parizadeh, Ahmed K. Ahmed, Christopher T. Gandia, Hal C. Davison, John V. Murray, Ian T. Mark, Ajay A. Madhavan, Darya Shlapak, Todd D. Rozen, Waleed Brinjikji, Prasanna Vibhute, Vivek Gupta, Kacie Brewer, and Olga Fermo

## ABSTRACT

**BACKGROUND AND PURPOSE:** CSF-venous fistulas (CVFs) associated with spontaneous intracranial hypotension (SIH) may have a transient appearance, relative to contrast arrival, which may influence the diagnostic performance of lateral decubitus CT myelography (CTM). We developed a dynamic CTM protocol using real-time bolus-tracking (dCTM-BT) to improve the temporal resolution and standardize the timing of CTM acquisitions post-intrathecal contrast administration. The purpose of our study was to evaluate the feasibility of the dCTM-BT technique and evaluate its diagnostic yield for CVF detection, stratified by brain MRI SIH findings.

**MATERIALS AND METHODS:** Patients with suspected SIH without extradural fluid collection on spine MRI who underwent dCTM-BT were retrospectively reviewed. CT bolus monitoring was performed at the upper thoracic level. Following the visualization of dense intrathecal contrast, at least 3 CTM acquisitions of the spine were obtained and reviewed by 2 neuroradiologists. The Bern SIH score was calculated on the brain MRI. The diagnostic yield for CVF detection was evaluated, stratified by Bern score categories and a receiver operating characteristic (ROC) analysis.

**RESULTS:** Out of 48 patients, 23 (48%) had a CVF on dCTM-BT, located at T1–5 ( $n = 4$ ), T6–12 ( $n = 18$ ), L1 ( $n = 1$ ), with 70% on the right. CVF was identified in 22/22 (100%) of patients who had a high Bern score, 1/7 (14%) of those who had an intermediate score, and 0/19 (0%) of those who had a low score. The area under the ROC curve was 0.99 (95% CI, 0.98–1.00). The optimal cutoff was a Bern score of  $\geq 5$  (96% sensitivity, 100% specificity).

**CONCLUSIONS:** dCTM-BT is feasible and has excellent diagnostic performance for CVF identification/localization. The Bern score is strongly associated with CVF detection and may help inform who will benefit from dCTM-BT.

**ABBREVIATIONS:** CTM = CT myelography; CVF = CSF-venous fistula; dCTM-BT = dynamic CT myelogram with bolus-tracking; DSM = digital subtraction myelogram; IQR = interquartile range; ROC = receiver operating characteristic; SD = standard deviation; SIH = spontaneous intracranial hypotension; SLEC = spinal longitudinal extradural CSF collection

Spinal CSF-venous fistulas (CVFs) are spontaneously occurring abnormal connections between a meningeal diverticulum or nerve root sleeve and an adjacent paraspinal vein that result in unregulated CSF egress and CSF volume depletion, commonly known as spontaneous intracranial hypotension (SIH).<sup>1</sup> The probability of identifying a spinal CSF leak source, including a CVF, is highly dependent on brain MRI findings that are systematically

incorporated into a 3-tier SIH score described by Dobrocky et al.<sup>2</sup> The identification and localization of a CVF are critical steps that are required for the successful treatment of SIH associated with CVF; however, these steps may be challenging, given absent findings on conventional myelography and that they require the use of specialized lateral decubitus myelographic techniques that are not routinely performed at many centers.<sup>3</sup>

Lateral decubitus digital subtraction myelography (DSM) is known to increase the yield of CVF detection by nearly 5-fold, compared to prone DSM.<sup>4</sup> While several centers use DSM as a first-line modality for CVF identification, lateral decubitus CT myelography (CTM) is increasingly being used, as it provides excellent cross-sectional spatial resolution for CVF detection, is an overall easier procedure for most operators to perform, and does not require general anesthesia.<sup>5–7</sup> However, a disadvantage of CTM, compared with DSM, is that its lack of temporal resolution potentially represents a significant limitation, as we have

Received May 17, 2023; accepted after revision October 29.

From the Departments of Radiology (T.J.H., D.P., A.K.A., C.T.G., H.C.D., J.V.M., P.V., V.G., K.B.), Neurology (T.D.R., O.F.), and Neurosurgery (T.J.H.), Mayo Clinic, Jacksonville, Florida; and Department of Radiology (I.T.M., A.A.M., D.S., W.B.), Mayo Clinic, Rochester, Minnesota.

Please address correspondence to Thien J Huynh, MD, MSc, Assistant Professor, Diagnostic and Interventional Neuroradiology, Departments of Radiology and Neurosurgery, Mayo Clinic, 4500 San Pablo Rd, Jacksonville, FL 32224; e-mail: huynh.thien@mayo.edu; @ThienHuynh15

Indicates article with online supplemental data.

<http://dx.doi.org/10.3174/ajnr.A8082>

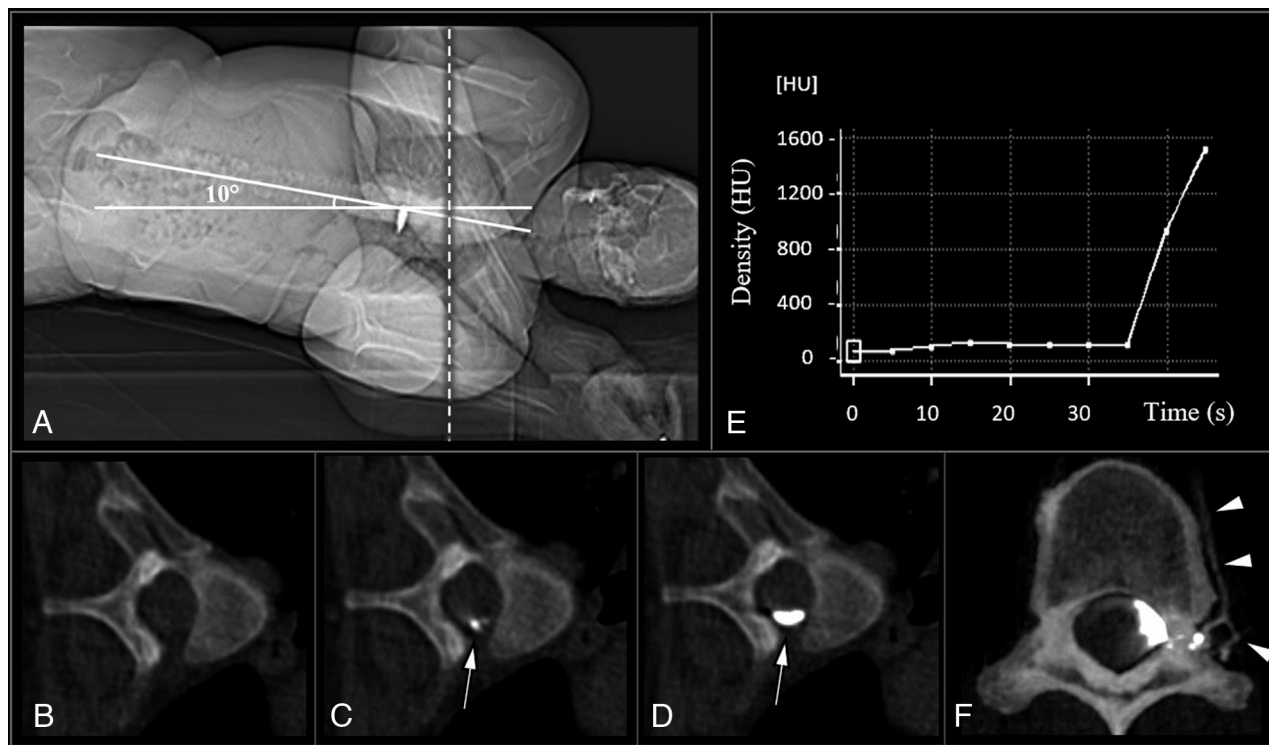


**FIG 1.** Lateral decubitus dynamic CT myelogram with real-time contrast bolus tracking (dCTM-BT): A, Frontal CT scout image shows patient in the left lateral decubitus position on the CT gantry table, with the hips placed at the apex of a custom firm foam wedge in the Trendelenburg position, at an angle of approximately 10°, to facilitate the caudocranial flow of contrast from the lumbar puncture towards the cervical spine. B–D, Real-time contrast bolus monitoring axial scans at the level of T5 (A, dashed line) with axial slices taken at 5-second intervals until the visualization of dense contrast (D, arrow). Note that dense contrast visualization is typically observed immediately after the initial appearance of contrast (C, arrow). E, Graph of density (Hounsfield units, HU) of monitored contrast bolus over time (region of interest placed at arrow in panels C and D; note that this graph is for illustrative purposes and is not utilized during the procedure). F, Axial CT myelogram showing the contrast enhancement of the paraspinal veins at the left T10, indicating a CSF-venous fistula (F, arrowheads).

anecdotally noted that several CVFs appear only transiently after contrast administration, which is a phenomenon that has recently been described using DSM<sup>8</sup> and has also been noted on CTM.<sup>7</sup>

Given the importance of the timing of contrast arrival, relative to CVF opacification, we sought to standardize the timing of CTM acquisition post-intrathecal contrast administration and improve upon the temporal resolution of conventional CTM by developing a lateral decubitus dynamic CTM protocol using real-time bolus-tracking (dCTM-BT). This technique helps ensure the consistent and standardized timing of dense contrast opacification along the length of the spine, and the multiple acquisitions add temporal resolution for CVF detection. The purpose of our study was to evaluate the feasibility of the dCTM-BT technique and evaluate its diagnostic yield for CVF detection, stratified by brain MRI SIH findings.

## MATERIALS AND METHODS

### Patient Population

Institutional Review Board approval was obtained, and the requirement for signed informed consent was waived.

Consecutive patients who were evaluated with dCTM-BT between March 2021 and December 2022 were retrospectively reviewed. The inclusion criteria for suspected SIH were based on the clinical criteria of the International Classification of

Headache Disorders, 3<sup>rd</sup> edition<sup>9</sup> and/or imaging findings on brain MRI. A spine T2-weighted MRI was performed on all patients as part of a systematic approach to SIH patient evaluation,<sup>10</sup> and patients with spinal longitudinal extradural CSF collection (SLEC) were excluded. All included patient records were reviewed for age, sex, and presenting symptoms.

### dCTM-BT Technique

A summary of the dCTM-BT protocol, including the effective dose estimates for each diagnostic CT acquisition, are listed in the Online Supplemental Data.

**Patient Positioning and Lumbar Puncture.** Lateral decubitus dCTM-BT was performed for all patients on 2 consecutive days, typically starting right side down on day 1 and followed by left side down on day 2. Two-day studies were performed, even if a CVF was found on the first day, to ensure a complete evaluation and exclude the possibility of multiple CVFs. The patient was positioned on the CT table in the lateral decubitus Trendelenburg position, with head downward and hips elevated, using angled foam wedges that place the patient at a 10–13° angle (Figure 1A). Pillows were placed under the patient's head and knees, and the arms were placed at or above the head, keeping the hands together for comfort to minimize motion artifacts. A frontal scout CT image of the patient was then reviewed to confirm Trendelenburg

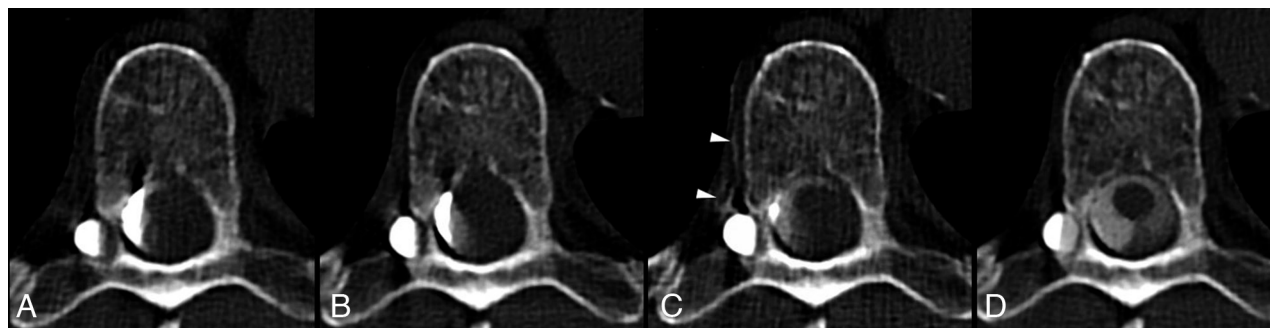


**FIG 2.** Axial images from a right lateral decubitus dynamic CT myelogram with bolus-tracking that were acquired at 30 seconds (A), 60 seconds (B), 2 minutes (C), and 4 minutes (D) after dense contrast was visualized on the bolus-tracking. A CSF-venous fistula is clearly identified on the image acquired at 2 minutes, with contrast visualized in a right T7 paraspinal vein (C, arrowheads). Note that the CVF only becomes more prominent after the adjacent diverticulum has nearly been completely filled with contrast.

spine angulation at a minimum of 5°, which will allow for the free cephalad flow of intrathecal contrast.<sup>5</sup>

Lumbar spine CT was then performed to guide needle access. A lumbar puncture was performed at or below the L2–3 level, using a 22-gauge spinal needle under CT fluoroscopy guidance. Intrathecal needle positioning was confirmed with CT fluoroscopy and with the return of CSF. If there was concern for needle placement, 0.5 mL of Omnipaque 300 (GE Healthcare) was injected to confirm positioning and avoid subdural injection. The specific equipment and injection techniques used, including the syringes and tubing, were similar to those described by Kim et al.<sup>5</sup> for lateral decubitus myelography, though we used a single contrast syringe with 10 mL of preservative-free iohexol contrast (Omnipaque 300). We injected 5–10 mL of preservative-free 0.9% saline prior to the contrast injection to ensure that there was no resistance to the injection and also to empirically provide positive pressure to encourage CVF visualization. The patients were confirmed to have either low or normal opening pressure, based on a lumbar puncture in the neutral lateral decubitus position either immediately prior to the performance of the dCTM-BT or on a prior lumbar puncture.

**Real-Time Bolus-Tracking and Dynamic/Multiphasic CT Acquisitions.** Bolus-tracking acquisitions are included in our CT software (Somatom Definition Flash; Siemens) and are widely used for contrast bolus monitoring for angiographic CT studies. The bolus-tracking pre-monitoring level was placed at the upper thoracic spine, typically T2 to T5, using the frontal and lateral CT scout images (Figure 1A). The bolus-monitoring intervals were set at 5 seconds per scan with manual triggering of the scan by the proceduralist. The rationale for placement in the upper thoracic spine was that due to the inherent delay from the time of bolus-tracking to the time of CTM acquisition, contrast would be expected to have just reached the cervical spine by the time of the first CTM acquisition. Initial pre-monitoring acquisition (Figure 1B) was performed and reviewed to ensure that the patient was not tilted either forward or backward, and, if needed, subtle patient adjustments were made. With the proceduralist in the room, bolus-tracking monitoring was then initiated, and 10 mL of iodinated contrast (Omnipaque 300) were hand-

injected at approximately 1 mL/second. During the injection, the proceduralist inspected the axial bolus-tracking acquisitions in real-time for confluent dense layering intrathecal contrast, which was typically >1500 HU in density and observed on the bolus-tracking scan immediately after the first appearance of contrast (Figure 1C, D). Once dense contrast was visualized, the proceduralist signaled to the CT technician to trigger the CTM acquisition, which was performed in a cranial-caudal direction to minimize the time to move from the level of the monitoring to the start of the acquisition level. We performed manual triggering for the scan with a qualitative assessment of the dense contrast as subtle patient movement. Often, only approximately 6–7 mL of contrast were injected by the time of the acquisition. In the rare event that contrast was not visualized during the real-time bolus tracking, a saline chase bolus, similar to that performed for DSM, was given to further encourage the cephalad flow of contrast.<sup>5</sup> At the time of the CTM acquisition, the proceduralist can either stay in the room or place the syringe setup in a sterile fashion on top of the patient and exit the room to reduce the radiation dose to the proceduralist. Following the initial CTM acquisition, which is typically acquired 15–30 seconds after the visualization of dense contrast on the bolus-tracking and thereby allows for the movement of the CT table, the remainder of the contrast was hand-injected. Additional CTM scans were performed 30–60 seconds (caudal-cranial acquisition direction) and 60–120 seconds (cranial-caudal acquisition direction) after the initial scan. The images were then reviewed for CVF visualization and the complete filling of the diverticulum, as we have anecdotally noted that a subset of CVFs only become visible after the complete filling of the adjacent diverticulum (Figure 2). Based on the diverticulum filling, additional scans were obtained at roughly 1–2 minute intervals. Each CTM acquisition was performed by covering the cervical, thoracic, and lumbar spine to the level of the lumbar puncture, with each acquisition lasting 10–20 seconds on a 128-slice CT scanner (Somatom Definition Flash). Each acquisition was also performed during instructed patient inspiration over 10–20 seconds to increase the conspicuity of the CVF.<sup>11</sup> Axial CT reconstruction was performed at a thickness of 0.6 mm, using bone and soft tissue kernels to allow for



**Patient and imaging characteristics with and without CSF-venous fistula<sup>a</sup>**

	Total (n = 48)	CVF Absent (n = 25)	CVF Present (n = 23)	P Value
Patient characteristics				
Age, mean (SD)	54 (12.0)	48 (11.5)	60 (9.7)	<.001
Female	37 (77.1)	18 (72.0)	19 (83)	.38
Orthostatic/Valsalva headache	35 (72.9)	17 (68)	18 (78)	.42
CVF characteristics				
Right side			16 (70)	
CVF level				
T1–T5			4 (17%)	
T6–T12			18 (78%)	
L1			1 (4%)	
MRI brain SIH findings				
Engorgement of venous sinus	21 (44)	0 (0)	21 (91)	<.001
Pachymeningeal enhancement	21 (44)	0 (0)	21 (91)	<.001
Suprasellar cistern effacement	26 (54)	7 (28)	19 (83)	<.001
Subdural fluid collection	1 (2)	0 (0)	1 (4.3)	.48
Prepontine cistern effacement	35 (73)	13 (52)	22 (96)	<.001
Decreased mamillopontine distance	33 (69)	12 (48)	21 (91)	.001
Bern SIH Score	4 (1–8)	1 (0–3)	8 (6–8)	<.001
Bern SIH score category				
Low	19 (40)	19 (76)	0 (0)	
Intermediate	7 (15)	6 (24)	1 (4)	
High	22 (46)	0 (0)	22 (96)	

<sup>a</sup>For the categoric variables, the data are presented as *n* (%) and are compared between groups via  $\chi^2$  or Fisher exact tests. For the continuous variables, the age is reported as a mean (SD) and is compared between groups via an independent *t* test, and the other continuous variables are reported as a median (IQR) and are compared between groups via a Mann-Whitney *U* test. A *P* value of <.05 was considered to be indicative of a statistically significant result and is reported in bold.

the detection of subtle CVFs. An example of multiple dynamic images obtained from a dCTM-BT study is shown in Figure 2.

### Imaging Review

All imaging was reviewed using a Visage viewer (v 7.1, Visage Imaging), using multiplanar reconstructions from the axial CTM source images, by 2 fellowship-trained, board-certified neuroradiologists. The presence and location of CVFs were identified by contrast in paraspinal veins, typically arising from the foraminal venous plexus. Two neuroradiologists evaluated contrast-enhanced MRIs of the brain and dCTM-BTs. For each examination, the MRI readers were blinded to the dCTM-BT findings, and the dCTM-BT readers were blinded to the MRI findings. Discrepancies were resolved by consensus.

For dCTMs, the readers reported: 1) the presence or absence of a CVF, 2) the side of the CVF, and 3) the level of the CVF. A single reader documented additional dCTM-BT details, including 1) the Trendelenburg spine angle on the lateral CT scout image, 2) adequate contrast layering throughout the spine on the initial CTM, 3) the number of CTM acquisitions, and 4) the presence of early renal contrast excretion.

For the brain MRIs, the readers reported the features of SIH based on the Bern SIH score.<sup>2</sup> These include 3 major findings (2 points each): Smooth pachymeningeal enhancement, engorged venous sinuses, and suprasellar cistern  $\leq 4.0$  mm; and 3 minor findings (1 point each): subdural fluid collections, prepontine cistern  $\leq 5.0$  mm, and mamillopontine distance  $\leq 6.5$  mm. Bern SIH scores of  $\leq 2$ , 3–4, or  $\geq 5$  points represent a low, intermediate, or high probability of identifying a spinal CSF leak, respectively. Radiation exposure was recorded as the volume-weighted CT dose index and dose-length product for each acquisition.

### Statistical Analysis

Continuous variables were reported as the mean (standard deviation [SD]) or median (interquartile range [IQR], 25–75) and compared between groups via an independent *t* test or Mann-Whitney *U* test, as appropriate for the data distribution. Categoric variables were reported as a frequency (percentage) and compared between groups via  $\chi^2$  or Fisher exact tests, as appropriate for the sample size. The interrater reliability for the Bern SIH Score and dCTM-BT evaluations were determined using weighted Cohen kappa ( $\kappa$ ). Agreement was defined as fair ( $\kappa = 0.21$ – $0.4$ ), moderate ( $\kappa = 0.41$ – $0.60$ ), substantial ( $\kappa = 0.61$ – $0.80$ ), or nearly perfect ( $\kappa = 0.81$ – $1$ ).<sup>12</sup> The diagnostic yield of the dCTM-BT was assessed overall and stratified by Bern SIH score. A receiver operating characteristic (ROC) analysis was performed to assess the association of the Bern SIH score with the CVF diagnosis and determine the optimal cutoff for CVF detection on dCTM-

BT. All tests were 2-sided, and a *P* value of <.05 was considered to be indicative of a statistically significant result. The statistical analyses were performed using R v4.1.2 (<https://www.r-project.org/>).

### RESULTS

Forty-eight patients with suspected SIH, with a mean age of  $54 \pm 12$  years (37 female, 77%), were evaluated with bilateral lateral decubitus dCTM-BT. The patients presented with orthostatic and/or Valsalva-induced headaches (73%), impaired balance (38%), tinnitus (33%), cognitive impairment (25%), and vision impairment (19%).

A single CVF was found in 23 of 48 (48%) patients, and none of the patients had multiple CVFs. The patient and CVF characteristics are summarized in Table. The patients with CVF were significantly older (mean of 60 versus 48 years,  $P < .001$ ). The CVFs were distributed in the thoracic and upper lumbar spine (range T3–L1), with most located at the level of T6–T12 (18/23, 78%) and on the right side (16/23, 70%). The readers had nearly perfect agreement in identifying the presence and location of CVF ( $\kappa = 0.88$ ; 95% CI, 0.77–0.99). The dCTM-BT was performed successfully in all patients, and all lateral decubitus studies (100%) had contrast visualized throughout the complete spine on the initial scan. The median (IQR) Trendelenburg spine angle was  $10^\circ$  ( $8^\circ$ – $12^\circ$ ). There was a median (IQR) of 4 (4–5) CTM acquisitions obtained for each complete lateral decubitus dCTM-BT study. Early renal contrast excretion was visualized in 4/23 (17%) of the studies with CVF present and in none (0/73, 0%) of the studies without CVF present ( $P = .003$ ). There was no significant difference between the spine angle tilt and the number of

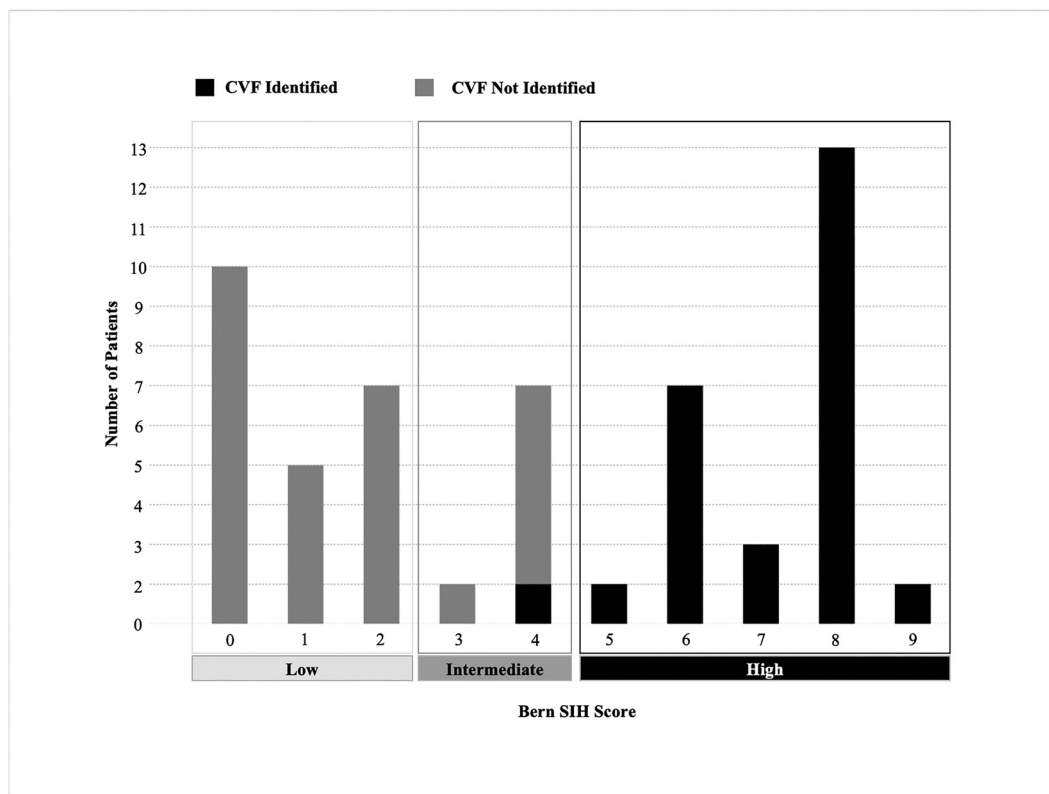


**FIG 3.** Bar chart illustrating the number of patients with CVF identified on dCTM-BT, across Bern SIH scores. The Bern SIH score was calculated based on the brain MRI, categorizing the probability of a spinal CSF leak as low (score of 0–2), intermediate (score of 3–4), or high (score of 5–9).

acquisitions, based on CVF presence. The median (IQR) effective dose estimate for each individual CTM acquisition was 25.3 (18.1–36.0) mSv, whereas the total dose for each complete lateral decubitus dCTM-BT was 97.6 (68.3–130.9) mSv. The total median (IQR) dose for each patient, including bilateral dCTM-BT, was 196.3 (150.7–267.7) mSv.

### MRI Brain SIH Findings

The median (IQR) Bern SIH score for all patients was 4 (1–8), and there was substantial interrater agreement ( $\kappa = 0.76$ ; 95% CI, 0.42–1.00). The median Bern SIH score (IQR) was 8 (6–8) among patients with CVF, which was significantly greater than the score of 1 (0–3) in those without CVF ( $P < .001$ ). As shown in the Table, all Bern SIH components were more common among patients with CVF ( $P < .001$ ), except for the presence of subdural fluid collection. However, this was possibly due to our limited number of patients with subdural collections. For all patients, the Bern SIH score tier was high in 22 (46%) patients, intermediate in 7 (15%), and low in 19 (40%).

### Diagnostic Yield of dCTM-BT, Stratified by Brain MRI Findings

Using the dCTM-BT technique, stratified by the Bern SIH score, CVF was detected in 100% (22/22) of the patients who had a high Bern SIH score, 14% (1/7) of those who had an intermediate score, and 0% (0/19) of those who had a low score (Figure 3). On the ROC analysis shown in Figure 3, the area under the curve for the association between the Bern SIH score and the identification of CVF on the dCTM-BT was 0.99 (95% CI, 0.98–1.00). The

maximum value of the Youden index was at a score of  $\geq 5$ . A Bern SIH score of  $\geq 5$  had a 96% sensitivity and a 100% specificity for the presence of CVF.

## DISCUSSION

We report the feasibility of performing lateral decubitus dCTM-BT and its high diagnostic yield for CVF detection, reaching 100% in the highest Bern SIH stratum and 48% in our overall cohort. The technique was successfully performed with contrast visualized throughout the spine on all CTM acquisitions. This allows proceduralists and patients to be confident in obtaining a high yield diagnostic study, despite variations in patient tilt due to the varying body habitus and morphology that are invariably encountered in patients with CVFs.<sup>13</sup> This technique also overcomes some of the limitations of traditional CTM, as the bolus-tracking allows for the consistent, reliable, and standardized timing of dense contrast opacification along the length of the spine, and the multiple/dynamic acquisitions add the needed temporal resolution required for optimal CVF detection. However, the high diagnostic yield of dCTM-BT should be carefully weighed against its relatively high radiation dose, especially with multiple acquisitions, and efforts should be made to limit its use to patients with high suspicion for SIH associated with CVF.

In our early experience with dynamic CTM and most recently described using DSM by Mark et al<sup>8</sup> it was noted that CVFs may often have a delayed appearance, relative to the timing of the contrast arrival, at the level of the CVF, ranging between 0 and 30 seconds, and it may appear only transiently, ranging from 24 to

68 seconds. Accordingly, if only a single CTM acquisition is performed either too early or late,<sup>7</sup> a subtle CVF may be missed, ultimately negatively impacting patient outcome. In theory, the dCTM-BT technique facilitates the “catching” of transiently appearing CVFs, as has been emphasized by Mamlouk et al,<sup>7</sup> and it is a natural evolution of the lateral decubitus CTM technique that was initially described by Kranz et al.<sup>6</sup> dCTM-BT may also be advantageous, compared to DSM, as the technique does not require general anesthesia, is more resistant to motion/cardiac pulsation artifacts, and has improved cross-sectional spatial resolution for the detection of subtle CVFs that are draining either intraosseously or into the internal vertebral venous plexus or are possibly being obscured by overlapping bony structures or a large diverticulum.

To our knowledge, this is the first study to report the diagnostic yield of CTM for CVF identification, stratified by the Bern SIH score. Previous studies have reported the overall diagnostic yields of DSM and CTM for CVF detection in SLEC-negative patients with SIH and have varied between 50% to 75%,<sup>4,7,10,14</sup> which is consistent with our overall yield of 48%. A recent study demonstrated the association of the Bern SIH score with the presence of CVF on lateral decubitus CT myelography; however, it did not evaluate the specific yield by Bern SIH score stratum.<sup>15</sup> While there are minor differences in the procedural techniques between studies, it is important to consider that the differences in the yields may be attributable to the pretest probability of CVF diagnosis of the patient cohort selected for DSM/CTM. Therefore, it is necessary to compare the diagnostic yield of CVF identification, stratified by Bern SIH score categories, instead of the overall yield, in order to determine the diagnostic performance of a modality. Only Kim et al<sup>14</sup> have reported the diagnostic yield of DSM for CSF leak, stratified by the Bern SIH score, in 62 SLEC-negative patients with SIH. In this study, 85% of the CSF leaks were from CVF, with an overall diagnostic yield of 53%.<sup>14</sup> Stratified by Bern SIH categories of high, intermediate, and low probability, DSM identified the site of the CSF leak in 67%, 46%, and 0% of cases, respectively. Our 100% diagnostic yield in the high-probability Bern SIH score category was considerably higher than the 67% CSF leak detection that was reported by Kim et al. Moreover, the higher area under the ROC curve for a Bern SIH score of 0.99 in our study, compared with 0.70 in the study by Kim et al, supports the greater diagnostic performance of dCTM-BT, compared with DSM. We suspect that the reason for the greater diagnostic performance is due to the improved cross-sectional spatial resolution combined with the added temporal resolution of the dCTM-BT technique, compared with DSM.

Interestingly, in both our study and the study by Kim et al<sup>14</sup> a Bern SIH score of  $\geq 5$  was the optimal threshold for the identification of a leak, with 96% sensitivity and 100% specificity for dCTM-BT versus 85% sensitivity and 52% specificity for DSM. This also corresponds precisely to the high-probability threshold established in the initial derivation and validation cohort that was established by Dobrocky et al.<sup>2</sup> Accordingly, this likely represents the ideal high-probability threshold in patients with SIH to support evaluation with either lateral decubitus DSM, CTM, or, ideally, dCTM-BT. The diagnostic yield in patients with intermediate scores varies widely, from 14% in our study to the

previously reported values of 46–73%.<sup>2,14</sup> The reason for the low yield in the group in our study remains uncertain; however, we suspect that this may be due to possible variations in interobserver agreement in the scoring of the various items of the Bern SIH score, which may be expected in practice. Understanding the reliability of each Bern SIH score component requires further dedicated study. For patients with a low Bern Score of  $\leq 2$ , our study, the study by Kim et al<sup>14</sup> and the internal validation cohort by Dobrocky et al<sup>2</sup> found a yield of 0%. Mamlouk et al<sup>7</sup> also reported a yield of 0% in 5 patients with normal brain MRI. Deciding whether to pursue lateral decubitus myelography in this cohort must be a highly individualized decision between the patient and the provider after a discussion of the risks and benefits, including the expected diagnostic yield. However, it is important to note that it has been reported in several studies that patients with normal MRI of the brain may still harbor a CSF leak,<sup>10,16,17</sup> and, even in the derivation cohort of the Bern SIH score, there was a 6.6% positive leak rate in the low-probability category.<sup>2</sup> The inability to identify a large portion of leaks in the intermediate and low Bern score groups remains uncertain and may be due to subtle, small, slow-flow and/or intermittently leaking CVFs that are below the resolution of conventional imaging.

The Bern SIH score was initially developed based on the probability of identifying a CSF leak source on conventional CT myelography and dynamic myelography among patients with suspected SIH.<sup>2</sup> One of the main limitations of the initial study was the generalizability of the score to predict the presence of a CVF, as the score was derived from CSF leaks between 2013 to 2017 at a single center, prior to the widespread use of lateral decubitus myelography for CVF detection.<sup>4,10</sup> Accordingly, especially given that epidural contrast leakage was primarily used to identify the presence of a CSF leak in the initial study, it is likely that patients with CVFs were largely excluded from both the initial score derivation and validation. Although this easy-to-use scoring has been applied as a diagnostic and/or post-treatment marker for SIH associated with CVF using both lateral decubitus DSM<sup>14,17</sup> and CTM,<sup>18</sup> its predictive performance has not yet been validated for CVF detection on dCTM-BT. With the outstanding discriminative ability of the Bern SIH score in our study of 0.99 AUC as well as the excellent sensitivity and specificity of a high score for CVF detection correlating with the high AUC in the derivation and validation cohorts of 0.98 and 0.93, respectively, our results validate this scoring system as a highly effective tool with which to triage patients with SIH associated with CVF for further evaluation with dCTM-BT.

Our study has several limitations. Our sample size was small, which limits statistical power and potentially introduces patient selection bias that could influence our results; however, our results and sample size are similar/larger, compared with prior publications.<sup>6,7,10,14</sup> All dCTM-BT was performed by a single proceduralist, which may affect the generalizability and dissemination of the results; however, this technique helps provide confidence to proceduralists by ensuring adequate contrast coverage and timing for the initial scans, and, ultimately, diagnostic performance, which should help support adoption. We only included the initial evaluation for patients without prior surgery or embolization. It is known that embolic material may cause

significant artifact, which may limit the visualization of a leak at the prior embolization site.<sup>3</sup> We also did not study same-day bilateral procedures;<sup>19</sup> however, we have since performed the dCTM-BT technique without difficulty in same-day bilateral procedures, and we expect a similarly high diagnostic yield. Further detailed study is needed to evaluate the yield by phase as well as the optimal timing and number of phases to be acquired. Our preliminary data suggest that the first 1 to 3 phases provided the highest yield, and we recommend performing at least 2 acquisitions and additional scans as needed to ensure the filling of large diverticula. The number of acquisitions and the greater radiation dose for CTM overall, compared with DSM,<sup>20</sup> should be balanced against its high diagnostic performance, the age of the patient, and local expertise. The improved efficacy of this technique, compared with non-bolus-tracked and single-phase CTM, also remains uncertain and requires further study. We included the complete cervical spine in our scan range; however, to reduce the radiation dose, the upper and mid cervical spine could theoretically be omitted, as CVFs are extremely rare in this location. It should also be noted that this technique does not evaluate CVFs in the lumbosacral region, which is known to harbor a small minority of leaks.<sup>21</sup> The further incorporation of photon-counting CT with this technique may also provide greater diagnostic performance with a lower radiation dose and is a promising avenue for further research.<sup>22</sup> We did not perform dedicated resisted inspiration in our study. The additional use of resisted inspiration may provide additional diagnostic yield; however, this also requires further study.<sup>23,24</sup> Spinal needles were used for the lumbar puncture in the study due to operator experience; however, it is universally recommended to use atraumatic needles for lumbar puncture, especially during the work-up of patients with SIH, to prevent post-dural puncture headaches and iatrogenic CSF leaks.<sup>25</sup>

## CONCLUSIONS

dCTM-BT is feasible and has excellent diagnostic performance for identifying and localizing CVFs associated with SIH. The yield approaches 100% in patients with the highest probability of harboring CVF, as categorized by the Bern SIH score. The Bern SIH score is strongly associated with the identification of a CVF in SLEC-negative patients with SIH and may be potentially used as a triage tool with which to identify patients who will benefit from dCTM-BT.

Disclosure forms provided by the authors are available with the full text and PDF of this article at [www.ajnr.org](http://www.ajnr.org).

## REFERENCES

- Schievink WI, Moser FG, Maya MM. CSF-venous fistula in spontaneous intracranial hypotension. *Neurology* 2014;83:472–73 [CrossRef Medline](#)
- Dobrocky T, Grunder L, Breiding PS, et al. Assessing spinal cerebrospinal fluid leaks in spontaneous intracranial hypotension with a scoring system based on brain magnetic resonance imaging findings. *JAMA Neurol* 2019;76:580–87 [CrossRef Medline](#)
- Kranz PG, Amrhein TJ. The promise and challenges of CSF-venous fistula treatment. *J Neurointerv Surg* 2022;14:951–52 [CrossRef Medline](#)
- Schievink WI, Maya MM, Moser FG, et al. Lateral decubitus digital subtraction myelography to identify spinal CSF-venous fistulas in spontaneous intracranial hypotension. *J Neurosurg Spine* 2019;31:902–05
- Kim DK, Brinjikji W, Morris PP, et al. Lateral decubitus digital subtraction myelography: tips, tricks, and pitfalls. *AJNR Am J Neuroradiol* 2020;41:21–28 [CrossRef Medline](#)
- Kranz PG, Gray L, Amrhein T. Decubitus CT myelography for detecting subtle CSF leaks in spontaneous intracranial hypotension. *AJNR Am J Neuroradiol* 2019;40:754–56 [CrossRef Medline](#)
- Mamlouk MD, Ochi RP, Jun P, et al. Decubitus CT myelography for CSF-venous fistulas: a procedural approach. *AJNR Am J Neuroradiol* 2021;42:32–36 [CrossRef Medline](#)
- Mark I, Madhavan A, Oien M, et al. Temporal characteristics of CSF-venous fistulas on digital subtraction myelography. *AJNR Am J Neuroradiol* 2023;44:492–95 [CrossRef Medline](#)
- Headache Classification Committee of the International Headache Society. The International Classification of Headache Disorders, 3rd edition (beta version). *Cephalalgia: An International Journal of Headache* 2013;33:629–808
- Farb RI, Nicholson PJ, Peng PW, et al. Spontaneous intracranial hypotension: a systematic imaging approach for CSF leak localization and management based on MRI and digital subtraction myelography. *AJNR Am J Neuroradiol* 2019;40:745–53 [CrossRef](#)
- Amrhein TJ, Gray L, Malinzak MD, et al. Respiratory phase affects the conspicuity of CSF-venous fistulas in spontaneous intracranial hypotension. *AJNR Am J Neuroradiol* 2020;41:1754–56 [CrossRef](#)
- Landis JR, Koch GG. The measurement of observer agreement for categorical data. *Biometrics* 1977;159–74 [Medline](#)
- Mamlouk MD, Shen PY, Jun P, et al. Spontaneous spinal CSF leaks stratified by age, body mass index, and spinal level. *AJNR Am J Neuroradiol* 2022;43:1068–72 [CrossRef Medline](#)
- Kim DK, Carr CM, Benson JC, et al. Diagnostic yield of lateral decubitus digital subtraction myelogram stratified by brain MRI findings. *Neurology* 2021;96:e1312–18 [CrossRef Medline](#)
- Callen AL, Pattee J, Thaker AA, et al. Relationship of Bern score, spinal elastance, and opening pressure in patients with spontaneous intracranial hypotension. *Neurology* 2023;100:e2237–46 [CrossRef Medline](#)
- Kranz PG, Gray L, Amrhein TJ. Spontaneous intracranial hypotension: 10 myths and misperceptions. *Headache* 2018;58:948–59 [CrossRef Medline](#)
- Brinjikji W, Garza I, Whealy M, et al. Clinical and imaging outcomes of cerebrospinal fluid-venous fistula embolization. *J Neurointerv Surg* 2022;14:953–56 [CrossRef Medline](#)
- Parizadeh D, Fermo O, Vibhute P, et al. Transvenous embolization of cerebrospinal fluid-venous fistulas: Independent validation and feasibility of upper-extremity approach and using dual-microcatheter and balloon pressure cooker technique. *J Neurointerv Surg* 2023;15:1234–41 [CrossRef](#)
- Carlton Jones L, Goadsby PJ. Same-day bilateral decubitus CT myelography for detecting CSF-venous fistulas in spontaneous intracranial hypotension. *AJNR Am J Neuroradiol* 2022;43:645–48 [CrossRef Medline](#)
- Nicholson PJ, Guest WC, van Prooijen M, et al. Digital subtraction myelography is associated with less radiation dose than CT-based techniques. *Clin Neuroradiol* 2021;31:627–31 [CrossRef Medline](#)



21. Mark IT, Morris PP, Brinjikji W, et al. **Sacral CSF-venous fistulas and potential imaging techniques.** *AJNR Am J Neuroradiol* 2022;43:1824–26 [CrossRef Medline](#)
22. Schwartz FR, Malinzak MD, Amrhein TJ. **Photon-counting computed tomography scan of a cerebrospinal fluid venous fistula.** *JAMA Neurol* 2022;79:628–29 [CrossRef Medline](#)
23. Mark IT, Amans MR, Shah VN, et al. **Resisted inspiration: A new technique to aid in the detection of CSF-venous fistulas.** *AJNR Am J Neuroradiol* 2022;43:1544–47 [CrossRef Medline](#)
24. Kranz PG, Malinzak MD, Gray L, et al. **Resisted inspiration improves visualization of CSF-venous fistulas in spontaneous intracranial hypotension.** *AJNR Am J Neuroradiol* 2023;44:994–98 [CrossRef Medline](#)
25. Uppal V, Russell R, Sondekoppam R, et al. **Consensus practice guidelines on postdural puncture headache from a multisociety, international working group: A summary report.** *JAMA Netw Open* 2023;6:e2325387 [CrossRef Medline](#)